Pol. J. Environ. Stud. Vol. 33, No. 3 (2024), 2103-2112
DOI: *10.15244/pjoes/172755* ONLINE PUBLICATION DATE: 2024-01-12

Original Research

Disturbance of Brain Metabolites in Mice: Potential Neuropathic Damage Mediated by Nanocarbon Black Exposure

Miaoyang Hu[1#], Muhan Li[1#], Xi Wang[1], Lei Jiang[2], Rong Gao[1], Tingwei Wang[3], Fei Huan[1], Wenwei Liu[4*]

[1]Key Laboratory of Modern Toxicology (NJMU), Ministry of Education; Department of Toxicology, School of Public Health, Nanjing Medical University, 211166, China
[2]Department of Emergency Medicine, the First Affiliated Hospital of Nanjing Medical University, 210029, China
[3]School of Food Science, State Key Laboratory of Food Science and Technology, Jiangnan University, 214122, China
[4]Department of Physical and Chemical Inspection,the Affiliated Wuxi Center for Disease Control and Prevention of Nanjing Medical University, 211166, China

Received: 22 July 2023
Accepted: 21 September 2023

Abstract

This Carbon black nanoparticles (CBNPs), a common and important manufacturing material, have been proven to exert adverse effects on brain function; however, the underlying neurotoxicity remains poorly understood. To unravel the deteriorating effect of CBNPs on the brain, a chronic long-term carbon black exposure mouse model (0 , 0.15 mg/ml, 0.5 mg/ml, 1.5 mg/ml groups) was established via nasal injection of CBNPs for 3 months. Intriguingly, the evidence directly showed the penetration of CBNPs in the brain, as the electron microscopic data showed an obvious deposition of CBNPs in various brain regions, where the mitochondrion displayed significant destruction. The metabolite changes based on GC/MS metabolic analysis displayed striking differences after CBNP exposure. With principal component analysis and the PLS-DA model, the brain metabolites of the control group and the treatment group were significantly distinguished, and these changes were involved in phenylalanine, tyrosine and tryptophan biosynthesis, D-glutamine and D-glutamate metabolism and linoleic acid metabolism. In detail, glutamine, glycine, lactic acid and norepinephrine, the excitotoxic metabolites, were markedly increased.

Collectively, the current study provides new insights into brain metabolic homeostasis after CBNP exposure, revealing potential targets in CBNP-induced neurotoxicity.

Keywords: nanocarbon black, metabolomics, neuropathic damage, neurotoxicity, amino acid

[#]Miaoyang Hu and Muhan Li contributed equally to this work.
*e-mail: liuwwcdc@126.com

Introduction

In recent decades, nanotechnology has rapidly developed, especially in the areas of electronics, engineering and biomedicine. Carbon black nanoparticles (CBNPs), with a primary size of 10-500 nm, have been widely used in manufacturing materials, such as rubber and printing [1]. During production, CBNPs are released into the atmosphere, presenting inhalation hazards for the general population. CBNPs are also considered a core constituent of some air pollutants, such as particulate matter (PM), which is associated with increased morbidity and mortality in respiratory and cardiovascular diseases [2]. The previous studies have demonstrated that inhaled CBNPs can enter the central nervous system through the blood circulation and olfactory nerves, posing adverse effects on the central nervous system [3-5].

Due to great surface area, CNBPs generate greater threats to public health. Laurie et al. found that inhaled ultrafine iron-soot reached the brain via the olfactory nerves and was associated with indicators of neural inflammation [6]. The pulmonary effects of CBNPs have been well documented [7]. In addition, CBNPs can induce systemic effects in organs remote from the primary site of exposure. For example, CBNPs have been proven to accelerate the progression of atherosclerosis1 and increase vascular disease risks [8]. Meanwhile, genotoxicity has been observed in the liver after pulmonary exposure to CBNPs [9]. For CBNP-associated developmental toxicity, prenatal exposure to CBNPs has been shown to increase the reactivity of the offspring immune system and induce neurodevelopmental changes [10]. Evidence suggests that CBNP exposure induced long-lasting diffuse perivascular abnormalities, including swollen astrocytic end-feet in the cerebral cortex [11]. He et al. demonstrated that exposure to CBNPs increases seizure susceptibility in male mice [3].

With primary cultured neurons, CBNP exposure has been revealed to induce significant neuronal damage, manifesting as decreased expression of the neuronal marker MAP2; meanwhile, CBNPs exposure results in excitotoxicity, which may be ascribed to the enhancement of the action potential frequency in neurons [3]. Our previous study also showed that CBNP treatment decreased cell viability, accompanied by an enormous increase in generation of reactive oxygen species [12]. In addition, oxidative stress, inflammation and apoptosis in CBNP-induced neuronal toxicity were also proven following in vivo exposure of chicken embryos [13]. However, the underlying mechanisms of neurotoxicity induced by CBNPs remain poorly understood.

Metabolomics, which is the profiling of metabolites in biofluids, cells and tissues, is routinely applied as a tool for biomarker discovery [14]. Metabolites are substrates and products of metabolism that drive cell function. The combination of chemical analysis, research technology, bioinformatics, and metabolomics is commonly used to solve human health problems [15]. In the present study, metabolomic analysis was applied to unravel the potential adverse effects of CBNPs on the mouse brain, which may provide novel insight into the neurotoxicity mediated by CBNPs.

Material and Methods

Animals and Treatments

Male BALB/c mice (n = 24, 8 weeks old) were used in all experiments which were obtained from Experimental Animal Center of Nanjing Medical University. Food and water were given ad libitum. The mice were housed in plastic cages under controlled environmental conditions (temperature: 18~22ºC, humidity: 30~50%) with a 12:12 h dark/light cycle. The mice were randomly divided into four treatment groups: the control group and the CBNPs treatment groups (0.15 mg/ml, 0.5 mg/ml, 1.5 mg/ml). CBNPs Printex 90 were freshly prepared each time. In the suspension, CBNPs were suspended in normal saline (NS) and were de-agglomerated with the ultrasonic water bath for 30 min after vigorous vortexed to make sure the homogeneity. Each animal in the experimental group were intranasally administered by placing a pipette tip with the dosing solution (20 µl) into the nostril of the mouse once a day for 3 months, and the control animals received an equal volume of vehicle (NS).

And the experiments were conducted under the control of the Ethics Committee of Animal Care and Experimentation of Europe and approved by the Institutional Animals Care and Use Committee (IACUC) at Nanjing Medical University (IACUC-1801008).

Reagents and Materials (Particles)

Acetonitrile was acquired from Merck & Co Inc. (USA), deuterated phenylalanine was obtained from CDN ISOTopes (Canada), methoxypyridine and N-methyl-N-(trimethylsilyl)trifluoroacetamide were purchased from Sigma-Aldrich (USA). Other chemicals were analytical grade.

The carbon black nanoparticle Printex 90 (14 nm primary particle size) was purchased from Orion Engineered Carbons (Borger, USA) and stored in dry and sterile conditions.

MRI Imaging Technology *in vivo*

After treatment, 7.0 T magnetic resonance imaging (MRI, Bruker BioSpin MRI, Germany) was used to image the brains of the mice. Mice were anaesthetized and maintained with 2% isoflurane by continuous inhalation. Heart rate, respiration rate and rectal temperature were continuously monitored by a life sign monitor. Scanning coronal position of mouse head with T2 sequence (TR 3000 ms, TE 45 ms). In this

experiment, the results were diagnosed and validated by two radiologists with over five years of work experience and they were blind to dose group.

Transmission Electron Microscopy Assay

After the neuroimaging studies, the mice were sacrificed, and the brains were immediately harvested and weighed.

The brains were collected and divided into three parts: the olfactory bulb, corpus striatum and hippocampus. The tissues were then immersed in 2.5% glutaraldehyde, after which the samples were rinsed 3 times with 0.1 M phosphoric acid for 15 min each time and postfixed in 1% osmium fixative for 3 hours. Subsequently, the brain tissues were immersed in 50% ethanol, 70% ethanol, 90% ethanol, 90% ethanol and 90% acetone (1:1) and 90% acetone for 20 min each at 4ºC and then immersed in a 100% acetone:embedding solution (2:1) volumetric mixture at room temperature for 4 h. Then, the brain tissues were immersed in 100% acetone:embedding solution (1:2) volumetric mixture at room temperature for 12 h, then immersed in pure embedding solution for 3 h at 37ºC, and subjected to a mixture of 100% acetone:embedding solution (1:2) volume for 12 h at room temperature and in pure embedding solution for 3 h at 37ºC and subsequently placed in the oven at 37ºC, 45ºC and 60ºC for 12 h, 12 h and 24 h, respectively. The sections were double-stained with 3% uranyl acetate and lead citrate. Finally, the slices were observed using a Japanese electronic JEM-1010 transmission electron microscope and photographed.

Brain Metabolic Extraction

Mouse brain samples were collected after dissection and stored in liquid nitrogen before analysis. The left half of the brain was placed in a 1.5 ml EP tube, and 800 µl of precooled 80% acetonitrile solution and an amount of deuterated phenylalanine were added. One steel ball (3 mm in diameter) was added to the EP tube, and the tissue was broken using a tissue crusher with a shaking frequency of 35 Hz for 15 min, which was repeated four times. The sample was centrifuged at 4ºC for 15 min at 12000 g after tissue fragmentation. A total of 300 µl of brain samples were concentrated and evaporated using a vacuum centrifuge concentrator, and 30 µl was mixed from the tissue supernatant of each sample to generate a sample pool for sample quality control (QC), divided into 300 µl per tube, and evaporated using a vacuum centrifuge. 70 µl of 20 mg/mL methoxypyridine solution was added after centrifugation, the mixture was vortexed for 2 min, and incubated at 80ºC for 40 min. After cooling to room temperature, 100 µl N-methyl-N-(trimethylsilyl)trifluoroacetamide (containing 1% TCMS, v/v) was used and incubated at 70ºC for 50 min. After centrifugation at 12000 rpm for 15 min at 4ºC, 150 µl supernatant was removed and placed in a sample bottle containing a liner tube for further analysis.

Brain Metabolite Measurement

Brain metabolites were detected using gas chromatography with time-of-flight mass spectrometry (GC-TOFMS, LECO, USA). A DB-5 MS (Agilent Technologies) fused silica capillary column (0.25 µm, 30 m × 250 µm) was employed for separation. The injector temperature was 280ºC, and the injection volume was 1 µl. The flow rate of helium carrier gas was kept at 1 ml/min. The initial column temperature was 80ºC and held for 4 min, ramped to 300ºC at a rate of 5ºC/min and held for 10 min. The ionization was carried out in electron ionization (EI) mode at 70 eV. Scan mass range (50-600 amu), scan rate 10 spectra/s, solvent delay time 4 min.

Multivariate Statistical Analysis

Multivariate statistical analysis was performed using Simca-P 14+ software, including principal component analysis (PCA) and orthogonal projections to latent structures-discriminant analysis (OPLS-DA). Cluster heatmap analysis was performed using the visual metabolomics analysis website Metaboanalyst 3.0 (http://www.metaboanalyst.ca). R code-based MetaMapp software was used for metabolic pathway analysis and the use of metabolic pathway analysis maps with CytoScape 3.4.0.

Statistical Analysis

SPSS 17.0 was used for statistical analysis. All experimental data are presented as means±SD unless otherwise noted. One-way ANOVA (one-way analysis of variance) was used to compare the quantitative data of multiple groups. Dunnett's t test was used for two-by-two comparisons between multiple groups. Origin, GraphPad Prism and R Studio (R i386 3.3.1) were used for figure generation.

Results and Discussion

CBNPs Exposure Exerts no Obvious Changes in Brain Structure and Weight

After exposed to Printex 90 for 3 months, body weight of mice haven't been affected by treatment. and then the animal MRI assay was performed. The T2 sequences of the olfactory bulb, corpus striatum and hippocampus were not significantly affected compared with the olfactory bulb, corpus striatum and hippocampus of the control group (Fig. 1A). In addition, the whole brain was weighed by analytical balance, and no significant difference was found between the brain mass of the CBNPs treatment groups and the brain mass of the control group. (Fig. 1B).

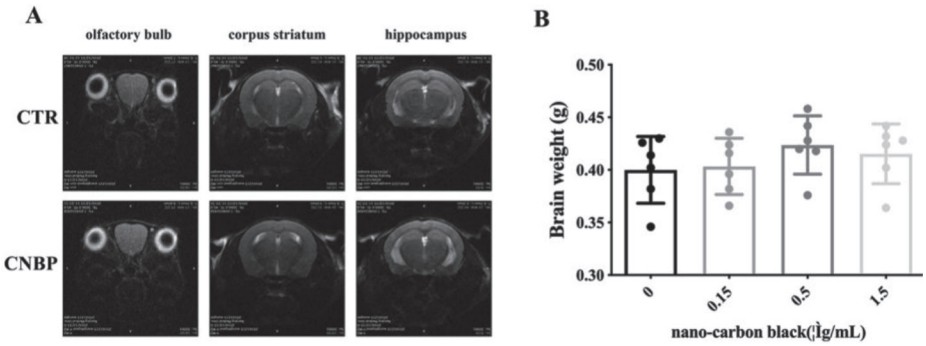

Fig. 1. General toxicity of CBNPs in the mouse brain. A) Brain MRI images of male C57 mice exposed to CBNPs. B) Brain weight of male C57 mice exposed to CBNPs.

CBNP Exposure Impairs the Ultrastructure of the Brain Region

To further examine the brain morphology after CBNPs exposure, transmission electron microscopy was used to observe the ultrastructure in several brain regions: the olfactory bulb, corpus striatum and hippocampus . After continuous CBNP exposure for three months, CBNPs were discovered to have a wide distribution throughout these brain regions. Notably, the mitochondrial cristae appeared disorganized and even disappeared in the CBNP treatment groups, documenting severe damage to mitochondrial structural integrity (Fig. 2).

Intergroup Differences in Metabolite Profiles Revealed by Principal Component Analysis

Having determined the adverse effects of CBNPs on mitochondria, which are important sites of carbohydrate and lipid metabolism, we examined metabolic homeostasis in the brain through GC/MS-based metabolite analysis.

As shown in Fig. 3, PCA score plots showed clear segregation between the four groups (R2X = 0.17, Q2 = 0.12). To further investigate the metabolic differences among these groups, the PLS-DA model was established. The scores of the CBNPs exposure groups were distinctly separated from the scores of the control group, indicating significant differences in the metabolome between the control and CBNP-exposed mice. To investigate the differentially abundant metabolites, a heatmap was generated, which clearly showed the alterations in the identified metabolites in the brain (Fig. 3E). The metabolites were screened, and the top 20 candidates were chosen with False Discovery Rate (FDR) principles. Similar to the results of PCA, the heatmap showed significant changes between the CBNPs exposure groups (0.5 mg/ml and 1.5 mg/ml) and the control group.

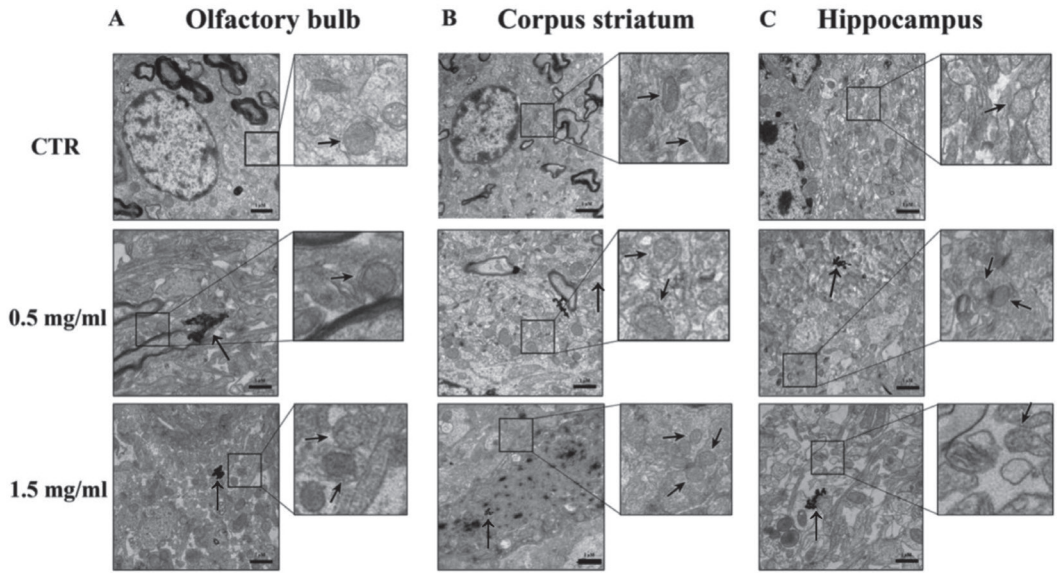

Fig. 2. A) Electron microscopic observation of the olfactory bulb of mice exposed to CBNPs (scale bar = 1 μm). B) Electron microscopic observation of the olfactory striatum of mice exposed to CBNPs (scale bar = 1 μm). C) Electron microscopic observation of the olfactory hippocampus of mice exposed to CBNPs (scale bar = 1 μm).

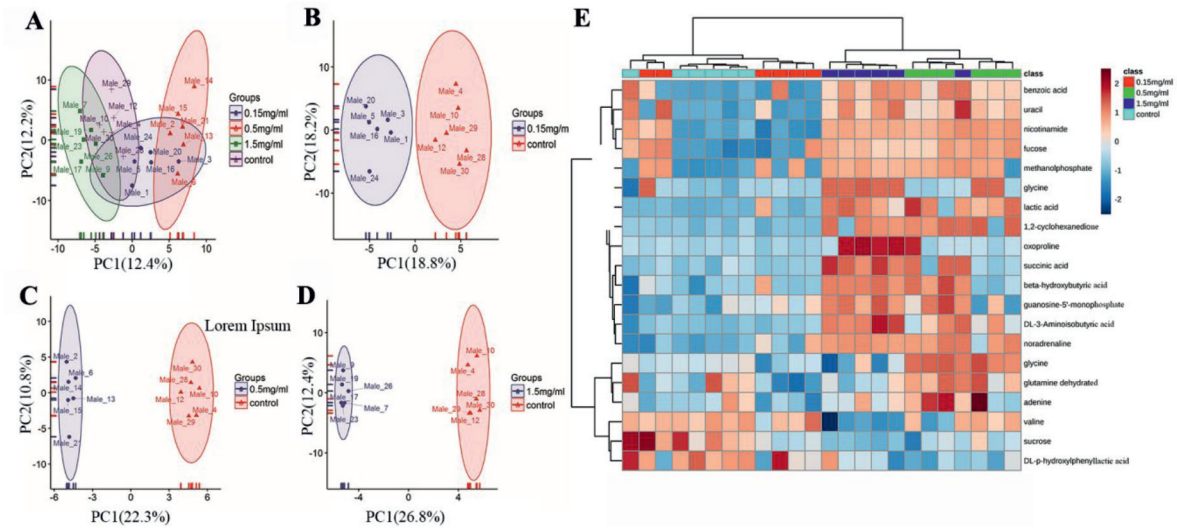

Fig. 3. Supervised principal component analysis OPLS-DA used for multivariate statistical analysis of brain tissue metabolites in mice treated with different doses for 3 months. A) principal component analysis of brain metabolites; orthogonal projections to latent structures-discriminant analysis (OPLS-DA) for B) control and 0.15 mg/ml nanocarbon black-exposed groups C) control and 0.5 mg/ml nanocarbon black exposure group D) multivariate statistical analysis for control and 1.5 mg/ml nanocarbon black exposure group: scatter is the GC/MS metabolite assay results for each sample group (n = 6); data were log-transformed and Pareto-scaled E) Hierarchical Pearson Clustering Heatmap Analysis.

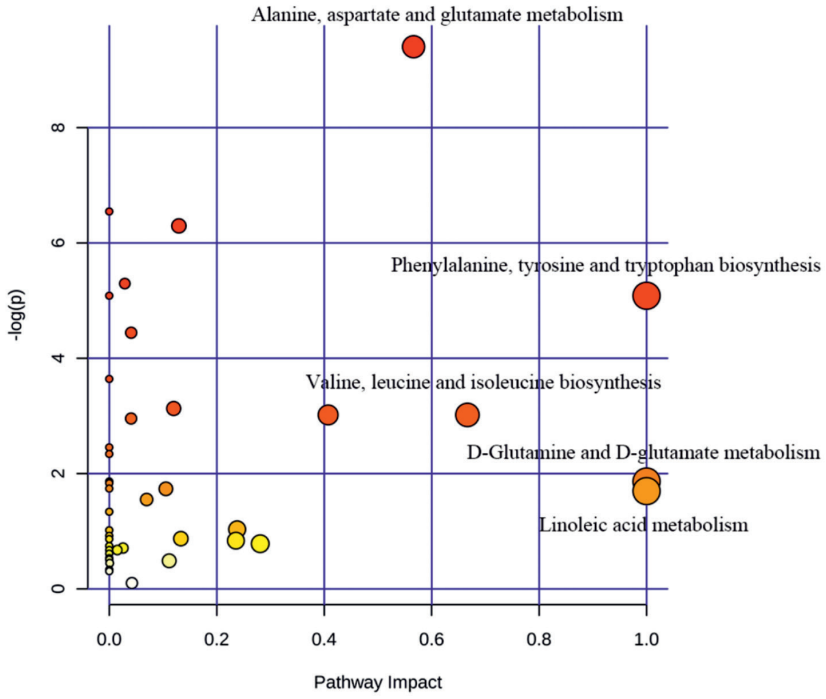

Fig. 4. Metabolic pathway enrichment analysis, screening metabolites with Fold Change value <0.5 or >2, x-axis represents the degree of influence of the metabolic pathway, the y-axis represents the degree of enrichment of metabolic pathway, the circle size and colour shade in the graph indicate the degree of enrichment and influence of each pathway, as well as brain metabolite pathway enrichment.

Metabolism Pathway Enrichment Analysis

To further explore the metabolic effects after CBNPs exposure, metabolic pathway enrichment analysis was carried out by MetaboAnalyst 3.0. Metabolic pathways with a fold change <0.05 or >2.0 were screened out. The results showed that phenylalanine, tyrosine and tryptophan biosynthesis, D-glutamine and D-glutamate metabolism and linoleic acid metabolism were obviously affected (Fig. 4). However, MetaAnalyst 3.0 does not support metabolic pathway integration analysis, suggesting further analysis of metabolic pathways.

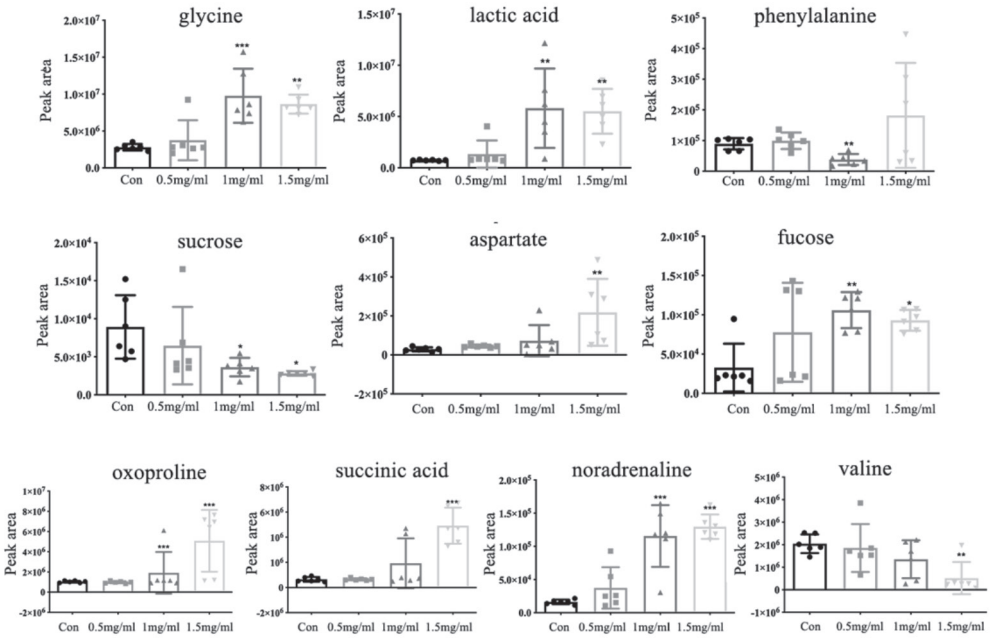

Fig. 5. Comparison of peak areas of brain metabolites within the four groups, metabolite screening using MS DIAL software with Fiehn mass spectrometry database, parameter VIP value>1, P<0.05, database comparison similarity >700; Dunnett-t test for significance between CBNP-dosed groups and control. (*P<0.05, ** P<0.01, *** P<0.001).

CBNPs Exposure Changes Brain Metabolites

Amino acids perform critical metabolic functions and are used for the synthesis of proteins, the formation of other low-molecular-weight compounds, and energy production by intermediate metabolites fueling other biosynthetic pathways [16]. To explore the differential changes in the identified metabolites between groups, the concentrations of metabolites in each group were compared. The results showed that the glycine, lactic acid aspartate, oxoproline, succinic acid and noradrenaline levels were significantly increased upon CBNPs exposure. We have improved the description of this results. In the levels of phenylalanine were markedly decreased after CBNPs treatment in the middle exposure group (0.5 mg/ml), valine level were significantly decreased in the high exposure group (1.5 mg/ml). Meanwhile , after CNBPs exposure, the fucose of mice in middle-dose(0.5 mg/ml) and high-dose (1.5 mg/ml) groups decreased significantly (Fig. 5).

Integration Metabolic Pathway Analysis

MetaMapp, a tool for integrating information from biochemical pathways and chemical and mass spectral similarity, was used [17]. The red nodes reflect the metabolites found to be upregulated, while those downregulated ones are shown in blue. Red edges denote Kyoto Encyclopedia of Genes and Genomes (KEGG) reactant pair links. Blue edges denote Tanimoto chemical similarity with T>700, clearly showing that 15 metabolites were significantly changed in the low exposure group (0.15 mg/ml) compared to the control groups, 8 metabolites showed a tendency of elevation and 7 metabolites were obviously decreased (Fig. 6B). Meanwhile, 18 metabolites were elevated in the middle exposure group (0.5 mg/ml), while 4 metabolites were decreased in the middle exposure group. (Fig. 6C). In the high exposure group (1.5 mg/ml), 29.03% (27/93) of the metabolites were significantly changed (Fig. 6D). Overall, 22 metabolites were markedly increased, while 5 metabolites were downregulated. In the CBNP-treated group, 4 pathways were enriched in the low exposure group, particularly the alanine, aspartic acid and glutamic acid metabolic pathways. Eleven metabolic pathways were significantly changed in the middle-dose exposure group, particularly phenylalanine, tyrosine and tryptophan biosynthesis. Phenylalanine metabolism, glycine, serine and threonine metabolism and niacin and niacinamide metabolism were also affected. Integrated metabolic pathway analysis also revealed that 13 metabolic pathways were significantly altered in the high exposure group, including glycine, serine and threonine metabolism; alanine, aspartate and glutamate metabolism; and valine, leucine and isoleucine biosynthesis (Fig. 6E).

As a primary component in air pollution, CBNPs have gained increasing attention due to their potential toxicity; therefore, a better understanding of the mechanism of CBNP-induced toxicity may allow for the appropriate regulation of potential health hazards. CBNPs can enter the central nervous system through blood circulation and olfactory nerves, affecting brain development and increasing neurological disease susceptibility [3].

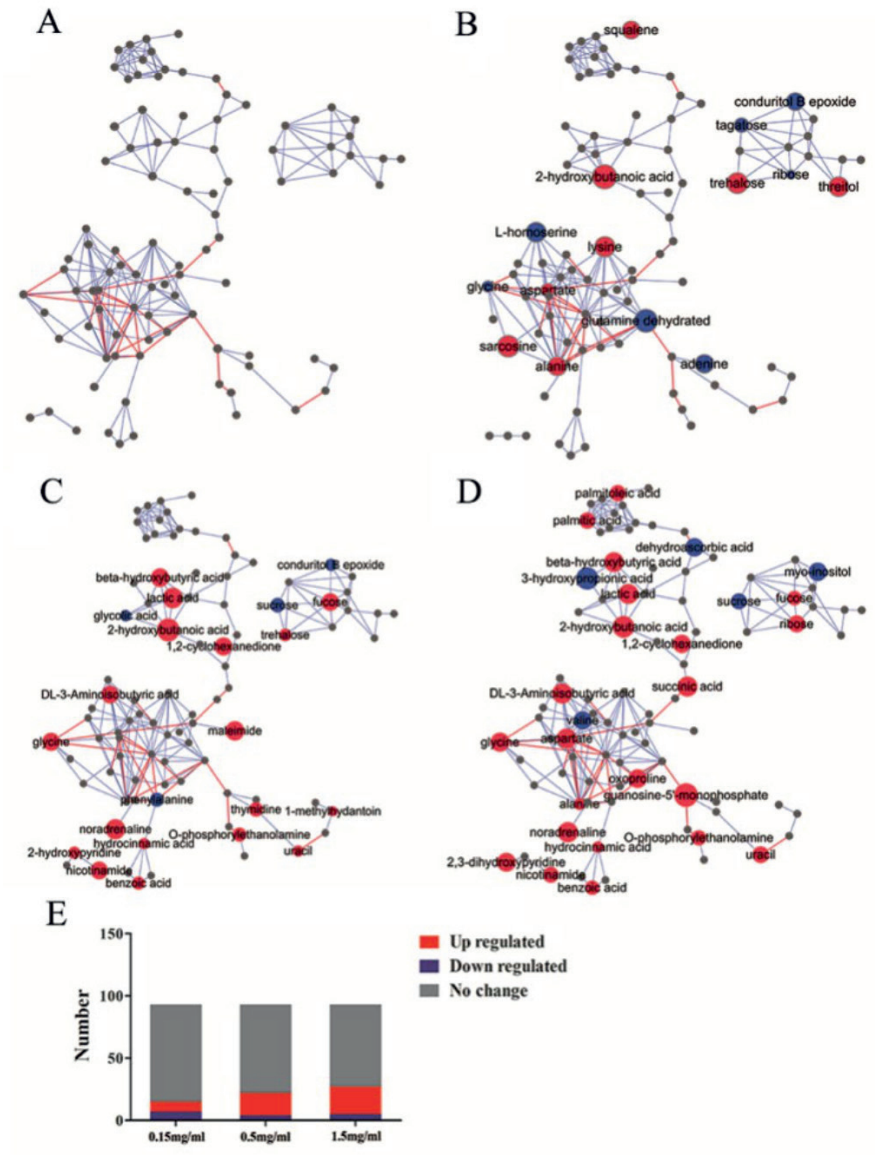

Fig. 6. Diagram of metabolic pathways of mouse brain metabolites. Metabolomic comparison between the A) blank control group, B) 0.15 mg/ml nanocarbon black-exposed group, C) 0.5 mg/ml nanocarbon black-exposed group, and D) 1.5 mg/ml nanocarbon black-exposed group. Metabolic pathways were generated by MetaMapp and mapped by CytoScape; red are upregulated metabolites, blue are downregulated metabolites, and grey are metabolites without statistical significance, calculated based on ploidy changes in MetaMapp; red lines are metabolic relationships between metabolites that can be looked up in KEGG, blue lines are metabolites according to PubChem provided by the size of the balls in the graph indicating the magnitude of the ploidy change values. E) Statistics of metabolite changes in the different dose groups.

In the present study, we investigated the neurotoxicity of CBNPs in the brains of mice exposed to the CBNP Printex90, which is often used as a model particle in toxicological research of particulate air pollution [18].

In a previous study, Printex90 was revealed to be distributed in the brain via system circulation [4]. To investigate whether chronic Printex90 exposure contributes to brain morphologic alteration, the MRI assay was exploited to scan the brain regions of the olfactory bulb, corpus striatum and hippocampus. However, the MRI assay revealed no significant changes in the CBNP exposure groups compared with the control group. Nonetheless, the detailed deciphering of CBNP-mediated neural damage using transmission electron microscopy revealed that the nanocarbon black particles were observed in all three brain regions of the 0.5 mg/ml and 1.5 mg/ml nanocarbon black-exposed groups accompanied by cellular substructure alterations (blurring and even disappearance of mitochondrial cristae) in the olfactory bulb, striatum, and hippocampus regions, strongly supporting the evidence that nanocarbon black directly enters the brain, resulting in the abnormal substructure of mitochondria, which may finalize neurotoxicology. Notably, once CBNPs enter the brain, they can be retained for a very long time, even for the entire lifespan [19]; thus, we suspected that CBNP-induced neurotoxicity may be in part due to the persistent accumulation of CBNPs in

the brain. Mitochondria are potential target organelles for CBNP-induced toxic effects [20]. Mitochondria are both the major intracellular source of oxidative stress, and mitochondrial dysfunction induces ROS generation [21]. Excess ROS production leads to impaired cognitive function in the brain, which facilitates neurodegeneration [22]. In the present study, we found a remarkable decrease or even disappearance of mitochondrial cristae in neural cells of the mouse brain after chronic CBNP exposure, suggesting that mitochondria may be an important target for CBNP neurotoxicity; therefore, metabolic homeostasis must be explored.

As expected, the PCA and OPLS-DA plots of the 0.5 mg/ml and 1.5 mg/ml exposed groups were more clearly separated with the increased dose, and the metabolic profiles were significantly different. Meanwhile, the metabolic heatmap also verified the aforementioned results, suggesting that CBNP exposure causes metabolic disturbance in the mouse brain.

To fully ascertain the changes in the metabolites in the mouse brain, the metabolites were analysed. Lactate is one of the main cerebral metabolites, and the presence of excess lactate levels indicates activated glycolysis in an oxygen-deficient environment where mitochondrial function is disrupted [23]. In support of our results, in the present study, we found obvious impairment of mitochondrial structure accompanied by markedly increased levels of lactate after CBNP exposure. This result suggested that CBNP exposure may cause hypoxia in some regions of the brain, which exacerbates the neurotoxic effects of CBNPs. Similar to gamma-aminobutyric acid, glycine is a well-known inhibitory neurotransmitter in the CNS [24]; glycine is an integral component of glutathione, the main antioxidant molecule of the cell. Therefore, glycine is required to maintain the cellular redox balance. In mitochondria, glycine fuels haem biosynthesis and thus sustains oxidative phosphorylation [25]. In the current work, the glycine level was significantly increased after exposure to CBNPs. We hypothesize that a hypoxic state of the brain, with impaired oxidative phosphorylation, was involved.

Phenylalanine is an indispensable amino acid that cannot be synthesized endogenously in the human body and therefore needs to be obtained from the diet. Phenylalanine is necessary for protein synthesis and is converted to tyrosine in cells [10]. Tyrosine is either used for protein synthesis, oxidized, or converted to important neurotransmitters, such as epinephrine, norepinephrine and dopamine [26]. In our study, the level of phenylalanine was significantly decreased. Aromatic amino acids in the brain function as precursors for the monoamine neurotransmitters serotonin and catecholamines [27]. As a consequence, the decline in these amino acid levels influences the rates of conversion to neurotransmitter products, contributing to neurotoxicity. To strengthen this effect, our previous study and other studies suggested that dysregulated tryptophan, phenylalanine and tryosine metabolism was closely associated with neuropsychiatric symptoms, such as depression [28]. These results suggest that CBNP exposure leads to metabolic disorders of phenylalanine, tyrosine and tryptophan.

Valine, leucine and isoleucine, the three essential amino acids, constitute the group of branched-chain amino acids (BCAAs). BCAAs are taken up to the brain parenchyma, where they serve several functions, such as as fuel material in brain energy metabolism [29]. In the current study, valine levels were significantly decreased in the brains of mice exposed to CBNPs, implying impaired energy metabolism after exposure to CBNPs. In the CNS, BCAAs play key roles in neurotransmitter synthesis, and disturbance of protein synthesis is implicated in neuronal diseases. Available results have shown metabolic disorders when BCAAs are in excess or limiting [30].

The fucose levels were also significantly increased in the brains of mice exposed to CBNPs, but the sucrose levels were decreased, suggesting a glycometabolic disorder after CBNP exposure. Fucose moieties on cell-surface glycans are increasingly recognized as critical to cell-cell interactions and signalling processes [31]. Fucose also ameliorates tryptophan metabolism and behavioural abnormalities in a mouse model of chronic colitis [32], and L-fucose can inhibit macrophage M1 polarization, inactivate the NLRP3 inflammasome and reduce the release of TNFα, IL-1β and IL-6 proinflammatory cytokines [33]. In the present study, the level of fucose was significantly decreased after exposure to CBNPs, suggesting the reduced protective effects of fucose in CBNP-induced neuropathnic damage.

Taken together, the current study directly proved that CBNP exposure contributes to the disturbance of metabolic homeostasis, characterized by the dysregulation of amino acid metabolism and glucose metabolism, which may provide novel clues for neuropathic damage after CBNP exposure.

Conclusions

In this study, a metabolomic approach was exploited to assess the potential toxicity of CBNPs in the mouse brain. The different metabolites induced by CBNPs were screened and indicated as potential biomarkers for CBNP exposure. Meanwhile, several metabolic pathways, such as amino acid and glucose metabolism, were involved in CBNP exposure, which may provide beneficial clues to unravel the toxic mechanism in CBNP-induced neural damage.

Conflict of Interest

The authors declare that there are no competing financial interests.

Acknowledgments

This work received financial support from the National Natural Science Foundation of China (82073584, 81701050, 81701872) and the Natural Science Foundation of Jiangsu Province (BK20191349).

Data Availability Statement

The data that support the findings of this study are available from the corresponding author upon reasonable request.

References

1. YAN J., LAI C.H., LUNG S.C., WANG W.C., HUANG C.C., CHEN G.W., SUO G., CHOUG C.T., Lin CH. Carbon black aggregates cause endothelial dysfunction by activating ROCK. J Hazard Mater. **338**, 66, **2017**.
2. TIN-TIN-WIN-SHWE, MITSUSHIMA D., YAMAMOTO S, FUKUSHIMA A., FUNABASHI T., KOBAYASHI T., FUJIMAKI H. Changes in neurotransmitter levels and proinflammatory cytokine mRNA expressions in the mice olfactory bulb following nanoparticle exposure. Toxicol Appl Pharmacol. **226** (2), 192, **2008**.
3. HE M., JIANG X., ZOU Z., QIN X., ZHANG S., GUO Y., WANG X., TIAN X., CHEN C. Exposure to carbon black nanoparticles increases seizure susceptibility in male mice. Nanotoxicology. **14** (5), 595, **2020**.
4. ZHANG Y., TU B., JIANG X., XU G., LIU X., TANG Q., BAI L., MENG P., ZHANG L., QIN X., ZOU Z., CHEN C. Exposure to carbon black nanoparticles during pregnancy persistently damages the cerebrovascular function in female mice. Toxicology. **422**, 44, **2019**.
5. UMEZAWA M., ONODA A. Maternal inhalation of carbon black nanoparticles induces neurodevelopmental changes in mouse offspring. Part Fibre Toxicol. **15** (1), 36, **2018**.
6. UMEZAWA M., ONODA A., KORSHUNOVA I., JENSEN ACØ, KOPONEN I.K., JENSEN K.A., KHODOSEVICH K., VOGEL U., HOUGAARD K.S. Repeated Iron-Soot Exposure and Nose-to-brain Transport of Inhaled Ultrafine Particles. Toxicol Pathol. **46** (1), 75, **2018**.
7. BOURDON J.A., HALAPPANAVAR S., SABER A.T., JACOBSEN N.R., WILLIAMS A., WALLIN H., VOGEL U., YAUK C.L. Hepatic and pulmonary toxicogenomic profiles in mice intratracheally instilled with carbon black nanoparticles reveal pulmonary inflammation, acute phase response, and alterations in lipid homeostasis. Toxicol Sci. **127** (2), 474, **2012**.
8. TANG J., CHENG W., GAO J., LI Y., YAO R., ROTHMAN N., LAN Q., CAMPEN M.J., ZHENG Y., LENG S. Occupational exposure to carbon black nanoparticles increases inflammatory vascular disease risk: an implication of an ex vivo biosensor assay. Part Fibre Toxicol. **17** (1), 47, **2020**.
9. EL-SAYED Y.S., SHIMIZU R., ONODA A., TAKEDA K., UMEZAWA M. Carbon black nanoparticle exposure during middle and late fetal development induces immune activation in male offspring mice. Toxicology. **327**, 53, **2015**.
10. ENNIS M.A., RASMUSSEN B.F., LIM K., BALL R.O., PENCHARZ P.B., COURTNEY-MARTIN G., ELANGO R. Dietary phenylalanine requirements during early and late gestation in healthy pregnant women. Am J Clin Nutr. **111** (2), 351, **2020**.
11. ONODA A., TAKEDA K., UMEZAWA M. Dose-dependent induction of astrocyte activation and reactive astrogliosis in mouse brain following maternal exposure to carbon black nanoparticle. Part Fibre Toxicol. **14** (1), 4, **2017**.
12. JIANG L., WANG T., XUE J., YU P., ZHANG J., WANG J. Nanosized carbon black exposure induces neural injury: effects on nicotinamide adenine dinucleotide phosphate oxidases and endoplasmic reticulum stress. J Appl Toxicol. **39** (8), 1108, **2019**.
13. SAMAK D.H., EL-SAYED Y.S., SHAHEEN H.M., EL-FAR A.H., ONODA A., ABDEL-DAIM M.M., UMEZAWA M. In-ovo exposed carbon black nanoparticles altered mRNA gene transcripts of antioxidants, proinflammatory and apoptotic pathways in the brain of chicken embryos. Chem Biol Interact. **295**, 133, **2018**.
14. JOHNSON C.H., IVANISEVIC J., SIUZDAK G. Metabolomics: beyond biomarkers and towards mechanisms. Nat Rev Mol Cell Biol. **17** (7), 451, **2016**.
15. TOKARZ J., HAID M., CECIL A., PREHN C., ARTATI A., MÖLLER G., ADAMSKI J. Endocrinology Meets Metabolomics: Achievements, Pitfalls, and Challenges. Trends Endocrinol Metab. **28** (10), 705, **2017**.
16. TABE Y., LORENZI P.L., KONOPLEVA M. Amino acid metabolism in hematologic malignancies and the era of targeted therapy. Blood. **134** (13), 1014, **2019**.
17. FAN S., SHAHID M., JIN P., ASHER A., KIM J. Identification of Metabolic Alterations in Breast Cancer Using Mass Spectrometry-Based Metabolomic Analysis. Metabolites. **10** (4), **2020**.
18. SEPULVEDA D., ROJAS-RIVERA D., RODRÍGUEZ D.A., GROENENDYK J., KÖHLER A., LEBEAUPIN C., ITO S., URRA H., CARRERAS-SUREDA A., HAZARI Y., VASSEUR-COGNET M., ALI M.M.U., CHEVET E., CAMPOS G., GODOY P., VAISAR T., BAILLY-MAITRE B., NAGATA K., MICHALAK M., SIERRALTA J., HETZ C. Interactome Screening Identifies the ER Luminal Chaperone Hsp47 as a Regulator of the Unfolded Protein Response Transducer IRE1α. Mol Cell. **69** (2), 238-252.e7, **2018**.
19. ZHANG S., MENG P., CHENG S., JIANG X., ZHANG J., QIN X., TANG Q., BAI L., ZOU Z., CHEN C. Pregnancy exposure to carbon black nanoparticles induced neurobehavioral deficits that are associated with altered m (6)A modification in offspring. Neurotoxicology. **81**, 40, **2020**.
20. DEWEIRDT J., QUIGNARD J.F., LACOMME S., GONTIER E., MORNET S., SAVINEAU J.P., MARTHAN R., GUIBERT C., BAUDRIMONT I. In vitro study of carbon black nanoparticles on human pulmonary artery endothelial cells: effects on calcium signaling and mitochondrial alterations. Arch Toxicol. **94** (7), 2331, **2020**.
21. YUAN X., NIE W., HE Z., YANG J., SHAO B., MA X., ZHANG X., BI Z., SUN L., LIANG X., TIE Y., LIU Y., MO F., XIE D., WEI Y., WEI X. Carbon black nanoparticles induce cell necrosis through lysosomal membrane permeabilization and cause subsequent inflammatory response. Theranostics. **10** (10), 4589, **2020**.
22. BELARBI K., CUVELIER E., DESTÉE A., GRESSIER B., CHARTIER-HARLIN M.C. NADPH oxidases in Parkinson's disease: a systematic review. Mol Neurodegener. **12** (1), 84, **2017**.
23. DIAZ F., RAVAL A.P. Simultaneous nicotine and oral contraceptive exposure alters brain energy metabolism and

exacerbates ischemic stroke injury in female rats. J Cereb Blood Flow Metab. **41** (4), 793, **2021**.
24. PARK S.J., CHOI J.W. Brain energy metabolism and multiple sclerosis: progress and prospects. Arch Pharm Res. **43** (10), 1017, **2020**.
25. DI SALVO M.L., CONTESTABILE R., PAIARDINI A, MARAS B. Glycine consumption and mitochondrial serine hydroxymethyltransferase in cancer cells: the heme connection. Med Hypotheses. **80** (5), 633, **2013**.
26. FERNSTROM J.D., FERNSTROM M.H. Tyrosine, phenylalanine, and catecholamine synthesis and function in the brain. J Nutr. **137** (6 Suppl 1), 1539S-1547S; discussion 1548S, **2007**.
27. STRASSER B., SPERNER-UNTERWEGER B., FUCHS D., GOSTNER J.M. Mechanisms of Inflammation-Associated Depression: Immune Influences on Tryptophan and Phenylalanine Metabolisms. Curr Top Behav Neurosci. **31**, 95, **2017**.
28. DENG Y., ZHOU M., WANG J., YAO J., YU J., LIU W., WU L., WANG J., GAO R. Involvement of the microbiota-gut-brain axis in chronic restraint stress: disturbances of the kynurenine metabolic pathway in both the gut and brain. Gut Microbes. **13** (1), 1, **2021**.
29. SPERRINGER J.E., ADDINGTON A., HUTSON S.M. Branched-Chain Amino Acids and Brain Metabolism. Neurochem Res. **42** (6), 1697, **2017**.
30. MURÍN R., MOHAMMADI G., LEIBFRITZ D., HAMPRECHT B. Glial metabolism of valine. Neurochem Res. **34** (7), 1195, **2009**.
31. LI J., HSU H.C., MOUNTZ J.D., ALLEN J.G. Unmasking Fucosylation: from Cell Adhesion to Immune System Regulation and Diseases. Cell Chem Biol. **25** (5), 499, **2018**.
32. BORISOVA M.A., SNYTNIKOVA O.A., LITVINOVA E.A., ACHASOVA K.M., BABOCHKINA T.I., PINDYURIN A.V., TSENTALOVICH Y.P., KOZHEVNIKOVA E.N. Fucose Ameliorates Tryptophan Metabolism and Behavioral Abnormalities in a Mouse Model of Chronic Colitis. Nutrients. **12** (2), **2020**.
33. HE R., LI Y., HAN C., LIN R., QIAN W., HOU X. L-Fucose ameliorates DSS-induced acute colitis via inhibiting macrophage M1 polarization and inhibiting NLRP3 inflammasome and NF-kB activation. Int Immunopharmacol. **73**, 379, **2019**.